Indonesian Journal of Electrical Engineering and Computer Science
Vol. 15, No. 3, September 2020, pp. xx~xx
ISSN: 2502-4752, DOI: 10.11591/ijeecs.v15.i3. ppxx-xx

A Simple Faulted Phase-Based Fault Distance Estimation Algorithm for a Loop Distribution System

Xxxxxxxxxxxxxxx
Xxxxxxxxxxxxxxx
xxxxxxxxxx.

Article Info

Article history:

Received Oct 1, 2018
Revised Dec 10, 2018
Accepted Jan 25, 2019

Keywords:

A. band pass filter,
B. discrete wavelets transform,
C. fault location,
D. loop distribution system,
E. noise,
F. traveling wave.

ABSTRACT (10 PT)

This paper presents a faulted phase-based traveling wave fault localization algorithm for loop distribution grids. This localization algorithm uses a band pass filter to remove noise from the corrupted signal. The arriving times of the faulted phase-based filtered signals can be obtained by using phase-modal and discrete wavelet transformations. The estimated fault distance can be calculated using the traveling wave method. The proposed algorithm presents detail level analysis using three detail levels coefficients. The proposed algorithm is tested with MATLAB Simulation single line to ground fault in a 10-kV grounded loop distribution system. The simulation result shows that the faulted phase time delay can give better accuracy than using conventional time delays. The proposed algorithm can give fault information accuracy up to 100% and fault distance estimation accuracy up to 99.7% with 30 dB contaminated SNR for the nearest lines from the measured terminal.

Corresponding Author:

Xxxxxxxxx

Xxxxxxxxxxx

xxxxxxxxxx

1. INTRODUCTION

Fault location on power system loop distribution network is very important to improve reliability for customer satisfaction and utilities. The outage location is needed to know accurately to remove the outage line quickly from the remaining parts of the system. Therefore, different conventional fault distance estimation methods are impedance-based method, high frequency and knowledge-based method, and traveling wave (TW) method.

Some researchers utilized impedance-based algorithms with the help of system fault signals [1]. Next, the knowledge-based method has been used to detect the fault location using neural networks, decision trees and support vector machine techniques [2-4]. Some previous researcher used voltage sag matching algorithm in [5], comparing faulty phase voltage with measure value approach was used in [6] and weighted least square approach in [7] respectively. All the above algorithms require training data sets with pre-defined different fault situations.

Traveling wave-based algorithms can give the best accuracy with the help of DWT filters [8-9]. Most of fault localization algorithms use the measured fault signals from single end of the system by identifying the first sudden changing point in the waveform [8-9]. This method was analysing in time domain that cannot get accurate arriving time for high impedance faults. A simple fault localization algorithm based on characteristics

of network topology and reclosure-generating traveling wave signals was introduced in [10]. However, the feeders without recloser cannot be protected by this algorithm.

The combination of impedance and traveling wave-based algorithms are proposed [11-12]. The arriving times of zero and aerial components are extracted by DWT filter (db4, level1) and utilized to estimate fault distance [11]. Dijkstra shortest path algorithm was proposed based on arrival time of initial voltage traveling wavefronts at the two terminals [12]. However, these algorithms did not consider about fault section to trip correctly the faulty part. Moreover, these methods utilized the general aerial mode arriving time of modal components which cannot give the accurate fault information for all fault types.

A decision tree aided traveling wave fault location algorithm was introduced in [13] and this algorithm used the two adjacent arrival times of the faulted line. This method could not get highest accuracy because it used the arriving time of general aerial mode components of Clark's transform which cannot give the accurate fault information for all fault types.

In addition, some single line to ground TW based methods used DWT filter and support vector regression (SVR) model [14], polarities of initial voltage and current signals [15], the difference of velocities by separating the initial arriving times of zero and aerial mode components [16] and the last one based on zero-sequence components distribution characteristics [17], respectively. These methods also used arriving time of conventional aerial mode that cannot give correct fault information for all faulted phases and fault types.

The next method is asynchronous voltage -based TW data fusion method [18]. This method requires the data training. Moreover, a single phase to ground fault localization method [19] used the fault characteristics include in zero sequence voltages and currents. However, the method is suitable for radial distribution systems.

According to literature reviews, the best accuracy can be achieved based on time delay between the first arriving times of detail coefficients of modal components of current traveling waves from the substation bus [14]. However, all the traveling wave methods applied in the above literature review used the arriving time of conventional aerial mode components. However, the arriving time of these components cannot give the accurate and correct fault information. Therefore, the proposed algorithm uses the arriving time of faulted phase-based modal component that can give higher accuracy than that of conventional methods with the consideration of noise effects, such as white noise.

The paper is organized as follows. Section 2 presents system process, Section 3 proposes noise filtering, Modal transform is explained in section 4. Wavelet transform is illustrated in section 5. Traveling wave method is presented in section 6. Section 7 focus on simulation results and discussions for loop distribution test systems. The last section is conclusion.

2.PROPOSED ALGORITHM

In this process, the recorded fault signals will firstly pass through the noise filter to remove noise from the input signal and then the filtered signals will be transformed to modal components to avoid mutual effects. In traveling wave fault location methods, the arriving times of fault signals are very important parameters to estimate fault distance, they can be extracted in time domain, sequence domain and wavelet domain as well. Therefore, the arriving times are extracted by using detail coefficients of discrete wavelet transform (DWT) in this paper. After that, the correct faulted phase is detected by using fault information accuracy content in the three-phase current signals. Finally, the estimated fault distance can be estimated by using time delays of detail coefficients of modal current components. The process is generally illustrated in Fig. 1.

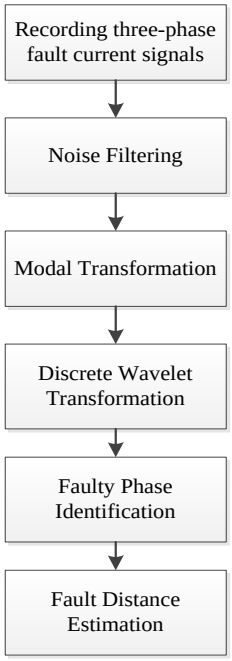

Fig. 1. Fault estimation process

The arriving times of absolute maxima of detail coefficient of zero and aerial mode current traveling wave signals can be estimated by using db6 mother wavelet because db6 mother wavelet can give more accurate arriving time than db4 mother wavelet that is used by most of previous fault location researchers for that purpose.

3. NOISE FILTERING

In order to simulate the effect of noise, white noise was added to the simulated signal. The smooth of input data has the objective of removing noise effect on the result of algorithm precision. Therefore, the noise cancellation procedures which apply a band pass filter is shown in the following Fig. 2. In this filter, firstly the white noise signal is added to the original signal. This corrupted signal is used as the input signal of band pass filter. Fig. 3 shows frequency ranges of zero and aerial mode components for the specified test system. According to frequency ranges of fault signals, the pass band frequency of the filter is 50 kHz to 1000 kHz to get correct fault information. The output of this filter will be used as the input of the following transformation processes.

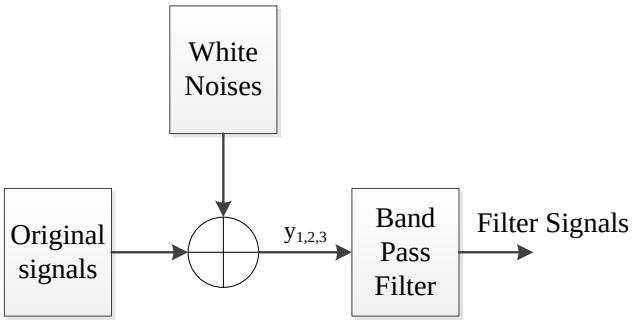

Fig. 2. Band pass noise filter

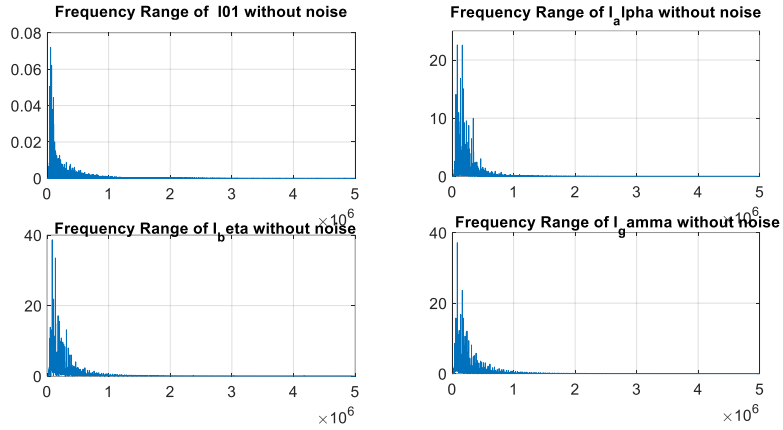

Fig. 3. Frequency Ranges of zero and aerial mode components

Table. 1. Filter Parameters

Filter Order	5
Cut off frequency	[50 1000] kHz
System Frequency	50Hz
Sampling Frequency	10MHz

4. PHASE TO MODAL TRANSFORM

In this section, the test system distribution lines are expected to be fully transposed. The phase components are necessary to transform to modal components to avoid mutual effects. Therefore, the Karenbauer's transform is used for that goal in this paper,

The matrix of Karenbauer's transform is a full-order matrix. An α -modal represents the "line" modal between phase "a" and phase "b". A β -modal represents the "line" modal between phase "a" and phase "c". A γ -modal the "line" modal between phase "b" and phase "c." Finally a 0-modal represents the residual value of three-phase current signals.

$$\begin{bmatrix} I_\alpha \\ I_\beta \\ I_\gamma \\ I_0 \end{bmatrix} = \frac{1}{3}\begin{bmatrix} 1 & -1 & 0 \\ 1 & 0 & -1 \\ 0 & 1 & -1 \\ 1 & 1 & 1 \end{bmatrix}\begin{bmatrix} I_a \\ I_b \\ I_c \end{bmatrix}, \quad (1)$$

where a, b, c represent the phase variables and $\alpha, \beta, \gamma, 0$ represent the modal variables. In this article, the most accurate arriving time of aerial mode is chosen from the aerial components related with Park's, Clark's and Karenbauer's transform, and aerial different component.

5. WAVELET TRANSFORM

The discrete wavelet transforms (DWT) splits into two components. They are approximation coefficients (cA) (low frequency) and detail coefficients (cD) (high frequency). Given a input signal *x*(k), its DWT can be calculated as follows:

$$DWT(m,n) = \frac{1}{\sqrt{a_0^m}}\sum_k x(k)\varphi\left(\frac{k - nb_0a_0^m}{a_0^m}\right), \quad (2)$$

where a_0 is the scale factor, b_0 is the translation factor, k is integer variable which refers to a sample number of an input signal, m and n are mother wavelet and decomposed level, respectively.

In this paper, detail coefficients of db6 mother wavelet for level1, 2 and 3 are extracted and utilized to reconstruct the signals. The arriving times are detected from the component that is combining the three reconstructed signals using combinations of three detail levels, D1, D2 and D3 to obtain accurate arriving time of the reflected fault signal. The accuracy comparison of db4 and db6 was described in [20]. To estimate fault distance using traveling wave method, in this paper, faulted phase-based time delay is utilized. It is necessary to get correct faulted phase from the fault information accuracy and faulted line from previous work [20]. Fig. 4. shows the three levels detail coefficients decomposition diagram.

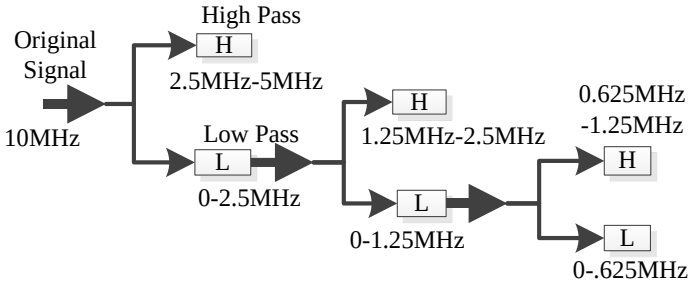

Fig. 4. DWT decomposition

6. TRAVELING WAVE THEORY

In the proposed algorithm, the recorded fault signals from the measure bus are transformed to modal components. The key to this paper is to use the arriving time delay between the reflected signals come from fault point to locate fault. Single ended fault location formula is given as follows [19]

$$d = \frac{v_0 v_1 (t_2 - t_1)}{(v_1 - v_0)}. \quad (3)$$

The time delay between zero mode current and aerial mode currents of Park's transform formula is shown in (4). The time delay between zero mode current and modal difference currents formula is shown in (5) and the time delay between zero mode and aerial mode current of Karenbauer's transform formula in (6)

$$\Delta t_d = t_0 - t_d, \quad (4)$$

$$\Delta t_{dq} = t_0 - t_{dq}, \quad (5)$$

$$\Delta t_{fp} = t_0 - t_{fp}. \quad (6)$$

The variable t_0 is the arriving time of the zero mode, which can be obtained using the residual current. The value can be calculated from

$$t_0 = \frac{d}{v_0}. \quad (7)$$

The zero-mode wave velocity can be estiamted based on the system characteristic impedance.

$$v_0 = \frac{1}{\sqrt{L_0 C_0}}, \quad (8)$$

where L_0 is the zero-sequence inductance and C_0 is zero sequence capacitance of the power line. The arriving time of the aerial mode using different transformation can be calculated using the same equation below.

$$t_d, t_{dq}, t_{fp} = \frac{d}{v_1}. \quad (9)$$

The wave velocity is given by:

$$v_1 = \frac{1}{\sqrt{L_1 C_1}}, \quad (10)$$

where L_1 and C_1 are positive sequence inductance and capacitance of the power line respectively. The arriving time of the aerial mode can be different depending on the transformation used to process the time domain signal. Using these different arriving times of aerial components can result different accuracies; therefore, the

modal difference component and faulted phase-based arriving time are used and compared with that of the conventional aerial mode components.

7. SIMULATION RESULTS AND DISCUSSIONS

In this paper, evaluation of fault type identification is performed on a power system simulation shown in Fig. 5. The test system consists of three power supplies of 33kV/10kV, 50Hz and a loop overhead distribution system (IEEE 14-bus modified test system). The faults are simulated in a km step on all branches of the test system. Before locating fault, the system firstly identifies the faulted line with the help of the fault detectors at all buses. Therefore, the fault detectors are installed at all buses of the test system. In this paper, the faulted section identification algorithm [20] is applied to get accurate faulted feeder. After obtaining faulty feeder, the system continues to estimate fault distance using only the recording signals from bus 1 (B1) for all lines of the test system. Various fault distances with fault resistance 0.001 Ω to 50 Ω considering noise effects with 70 to 30 SNR dB are simulated and analysed as well. Total 1650 cases for 55 points with 100 iterations for every case are studied.

System parameters are generator source resistance 13.96 Ω and source inductance of 0.35H. Distributed line parameter model is used as overhead distribution line parameters.

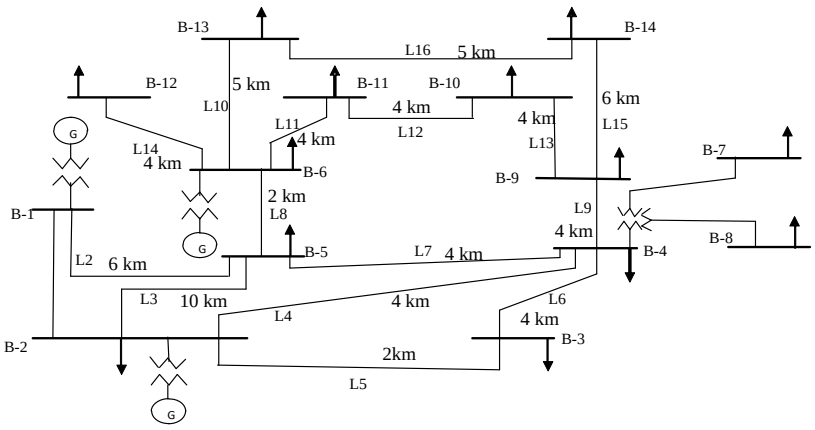

Fig. 5. IEEE 14-Bus modified test system [20]

7.1. Accuracy Calculation

In the loop distribution system, there are many possible predefined fault distance values because there are many paths from the fault location to the measure terminal. For example, when a fault occurs at the middle of line (L7) which is 4 km long, there are five possible ways to get different five arriving signals from the fault point (F) to the measure terminal (B_1). They are shown in the following Fig. 6.

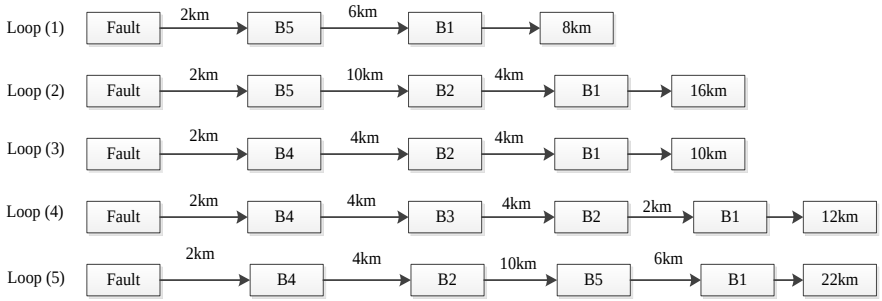

Fig. 6. Possible actual fault distances when fault occurs at L_7

According to these loops, possible fault distances from the measuring point are 8, 16, 10, 12 and 22km that are possible actual fault distances for that case. Hence the range of possible fault distance (PFD) in this case is between 8 and 22 km. If the estimated fault distance (EFD) resides within the possble fault distance, the estimated fault distance is feasible. Otherwise, the algorithm assumes that the estimated distance is erronous and should be discarded. This scenario can occur under noisy environment.

In the accuracy calculation process, the algorithm defines the range of possible fault distance (PFD) according to faulted line and then check whether the estimated fault distance (EFD) is within PFD range or not. If EFD is within the PFD range, the calculated fault distance is kept for further calculation.

To assess the algorithm performance under random noisy environment, each fault point is simulated for 100 times. We define two parameters to show the performance of the algorithm. Those parameters are Fault Inforamtion Accuracy (FAC) and Fault Distance Estimation Accuracy (FDEAC).

The Fault Inforamtion Accuracy is defined by

$$\text{FAC}=\frac{\text{feasible distance cases}}{\text{total iteration}}\times 100\% , \tag{11}$$

where feasible distance cases are number of cases that the estimated fault distance (EFD) falls within the possible fault distance range (PFD) and the total iteration is the number simulation done at that location.

The Fault Distance Estimation Accuracy is defined by

$$\text{FDEAC}=\left(1-\left|\frac{\text{AFD-AEFD}}{\text{AFD}}\right|\right)\times 100\%. \tag{12}$$

This FDEAC shows the averaged accuracy under the simulation. The higher the FDEAC value, the more accurate the esimation is.

According to the example shown in Fig. 6, the actual fault distance can have multiple values depending on the path the traveling wave take. Therefore, the algorithm must choose the possible fault distance from the list to calculate the accuracy value. In this paper, the value closest to the average estimated fault distance is chosen. If there are two possible AFD values, the smallest one is chosen.

For example, in the case of signals mixed with noise 60 SNR dB, number of count (FAC) is 100 % and the AEFD is 7.9908km. Therefore, the AFD is 8km because it is the closest one with AEFD for that case. The fault distance estimation accuracy is 99.89% by (12).

7.2. Arriving Time based on Faulted Phase

The arriving times of detail coefficients of zero and aerial mode current components are shown in Fig. 7 when phase ‘c’ to ground fault occurs. In this figure, the arriving times of the three aerial mode components are not the same because the impedances of these three aerial components are different due to fault. When phase ‘c’ to ground fault occurs in the system, the arriving time of α -modal component related with healthy phases differs from that of β and γ modal components related with faulted phase. Therefore, the proposed algorithm used the arriving time of faulted phase related modal component to get higher accuracy.

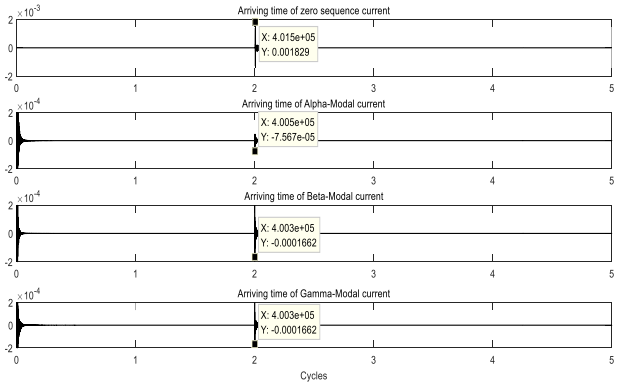

Fig. 7. Arriving times of detail coefficients of zero and aerial mode components when a single line to ground (CG) fault occurs at L7

7.3. Detail Level Analysis without Noise

The arriving times of fault signals, such as zero and aerial mode components are needed to be more accurate to get better accuracy than conventional methods. In this paper, the detail coefficients using db6 mother wavelet for three detail levels are extracted and utilized to reconstruct signals. After that, FDEAC for all lines are tested by changing different detail levels and compared to choose the suitable detail component that can give better accuracy and noise reduction performance. The cases are the arriving times taken from (i) the combination of reconstructed signals by using detail coefficients level1 (D1), level2 (D2) and level3 (D3) shown here as D123 (ii) the combination of reconstructed signals by using detail coefficients, D1 and D2, shown here as D12 (iii) the reconstructed signals by using detail coefficients, D1, (iv) the reconstructed signals

by using detail coefficients, D2, and (v) the reconstructed signals by using detail coefficients, D3, respectively. In this study, the proposed algorithm is tested with single line to ground (SLG) fault for all lines of test system.

Table. 2. Average FDEAC for all lines with different detail levels without noise effects

Faulted Lines	FDEAC (%) by				
	D1+D2+D3	D1+D2	D1	D2	D3
L1	99.68	99.68	99.90	0.00	98.19
L2	99.75	99.97	99.68	99.68	98.90
L3	99.91	93.53	93.62	93.81	94.66
L4	99.82	99.82	85.91	99.82	99.68
L5	99.68	99.81	99.98	99.64	0.00
L6	99.89	99.58	99.79	99.79	85.52
L7	99.89	94.44	94.27	99.999	0.00
L8	99.91	99.83	99.91	63.17	99.19
L9	99.85	99.98	99.94	98.34	94.99
L10	99.85	99.98	99.93	99.98	99.65
L11	99.85	94.11	99.94	94.76	0.00
L12	99.92	95.63	95.63	98.48	99.92
L13	95.85	93.90	96.86	93.90	0.00
L14	99.85	88.52	99.94	88.52	0.00
L15	99.88	96.10	95.05	99.78	99.83
L16	99.92	97.50	99.997	97.50	0.00
Average	99.59	97.02	97.52	95.14	97.05

Table 2 shows the performance of FDEAC for all lines of the test system without noise in the simulation. The FDEAC using the time delay with combination of the fault information from the detail level 1,2,3 (D123) can give the best accuracy in five comparative cases.

7.4. Detail Level Analysis with Noise

According to Fig. 8 and 9, although FAC and FDEAC by D_1 are the best in overall, the values are not significant in single case for five parameters with different detail levels. However, the parameter with combination of detail level 1,2,3 can give better accuracy in high noise levels, such as 30dB, 40dB and 50dB and the fault distance estimation accuracy by using this parameter for most of faulted lines are above 99%. Therefore, the arriving times for proposed fault distance estimation algorithm can be detected from the component that is a combination of reconstructed signals by using detail coefficients level 1, level 2 and level 3 (D_1+D_2+D_3) of db6 mother wavelet.

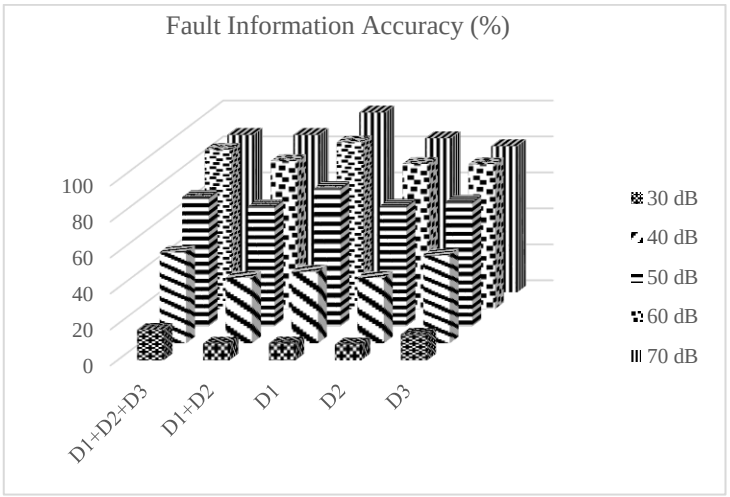

Fig. 8. Performance of average fault information accuracy for all lines with different detail levels

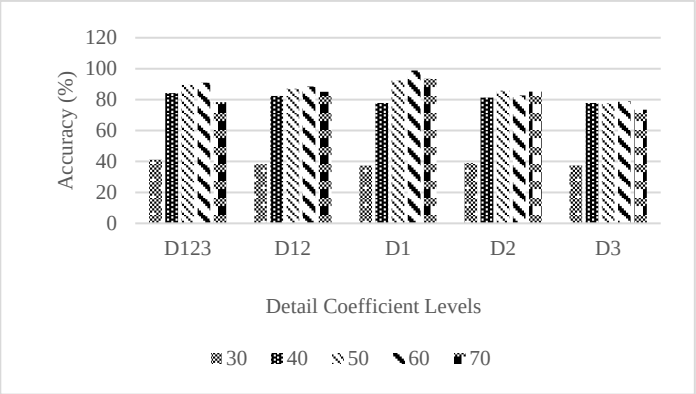

Fig. 9. Performance of average fault distance estimation accuracy for all lines with different detail levels under different noise levels

7.5. Performance of Proposed Algorithm Accuracy

The fault information accuracy can get from the value of count over 100 iterations. Count is numbers of possible fault distance value included in the estimated data. The possible fault distances are the lengths between minimum and maximum possible lengths that are defined according to faulted line.

For example, when a fault occurs at the L_7, the possible fault current loops are shown in Fig. 6. In that case, the minimum possible fault distance (d_1) is the minimum value from the measured terminal to fault and the maximum possible length (d_2) is the maximum length from the measured terminal to fault. In this paper, the deviation for the possible fault distance range is ± 0.5 km.

The performance of average fault information accuracy and average fault distance estimation accuracy for L_1 are shown in Table 3 and 4 as examples for all lines. Because the test results for all lines are very similar with that of L_1. In Table 3, the average fault information accuracies of five time delays, such as Δt_{dq}, Δt_d, Δt_α, Δt_β and Δt_γ for L_1 are compared. The fault information accuracy comes from number of possible estimated fault distance that included in estimated data with respect to proposed algorithm for each SNR value. According to the result in Table 3, it can be seen that Δt_{dq} gives better fault information accuracy than conventional time delay, Δt_d for L_1 because Δt_{dq} comes from arriving times of zero modal and aerial difference component (I_{dq}) related with three phases. However, if the faulted phase-based algorithm is used, it can get the best accuracy in these three-time delays up to 30 dB SNR.

According to Table 3, the proposed method can be used to make double check for choosing accurate faulted phase based time delay by using the pattern of fault information accuracy of three modal time delays, Δt_α, Δt_β and Δt_γ. When phase 'a' to ground (AG) fault occurs in the system, the fault information accuracy from using the time delay of the healthy phase Δt_γ is lower than others.

If we observe the fault distance estimation accuracy of the phase 'a' to ground (AG) fault in Table 4, higher accuracy can be obtained from the time detay of the faulted phase, which are Δt_α and Δt_β in this case. The algorithm can choose to use either time delay with similar accuracy perforamnce.

Table 3. Performance of fault information accuracy of proposed fault localization algorithm for L1

F.T	SNR (dB)	Δt_{dq}	Δt_d	Δt_α	Δt_β	Δt_γ
AG	30	100	100	100	100	2
	40	100	100	100	100	0
	50	100	100	100	100	1
	60	100	100	100	100	3
	70	100	100	100	100	2
BG	30	1	1	0	1	0
	40	8	3	13	3	13
	50	100	3	100	2	100
	60	100	7	100	2	100
	70	100	99	100	3	100
CG	30	3	100	3	100	100
	40	98	100	2	100	100
	50	100	100	0	100	100
	60	100	100	4	100	100
	70	100	100	2	100	100

Table 4. Performance of fault distance estimation accuracy of proposed fault localization algorithm for L1

F.T	SNR (dB)	Δt_{dq}	Δt_d	Δt_α	Δt_β	Δt_γ
AG	30	99.880	99.955	99.488	99.977	72.632
	40	99.562	99.511	99.536	99.511	50.481
	50	99.281	99.281	99.281	99.281	32.305
	60	99.255	99.255	99.255	99.255	69.437
	70	99.255	99.255	99.255	99.255	-
BG	30	31.100	26.626	31.800	13.846	93.503
	40	98.046	47.925	94.051	13.846	99.147
	50	99.836	73.908	99.881	18.958	99.856
	60	99.634	91.267	99.664	89.672	99.664
	70	99.281	98.398	99.281	82.004	99.281
CG	30	97.871	99.561	40.044	99.638	98.484
	40	98.790	99.792	22.366	99.792	99.792
	50	99.098	99.255	0.000	99.255	99.255
	60	99.255	99.255	36.620	99.255	99.255
	70	99.255	99.255	49.096	99.255	99.255

In Table 4, the performance of average fault distance estimation accuracy and the maximum average accuracy can get up to 99.98% with SNR= 30 dB. For the average fault distance estimation accuracy, the estimated values with the number of counts less than 10 are neglected and not used to calculate accuracy for that point.

Fig. 10 shows that the performance of average fault distance estimation accuracy for all lines with the impact of noises (30-70 dB SNR values). In these figures compare the average fault distance estimation accuracy (FDEAC) using conventional time delay Δt_d , aerial difference time delay Δt_{dq} and proposed faulted phase time delay Δt_{fp} , respectively.

According to the result shown in Fig. 10, the fault distance estimation accuracy using the time delay of the faulted phase ($FDEAC_{fp}$) shows the best over all accuracy. Hence, the time delay of the faulted phase should be used to calculate the fault distance.

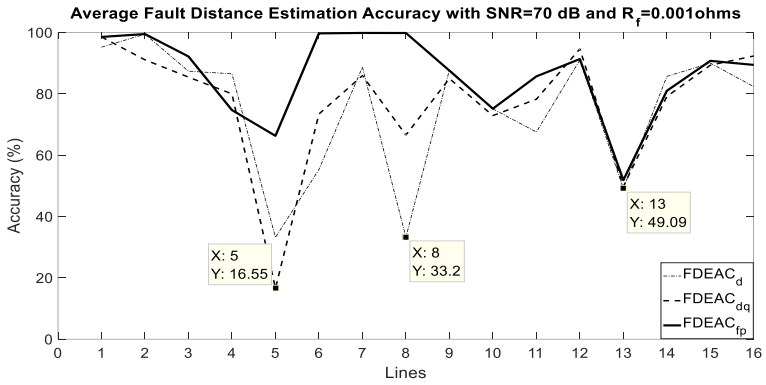

(i)

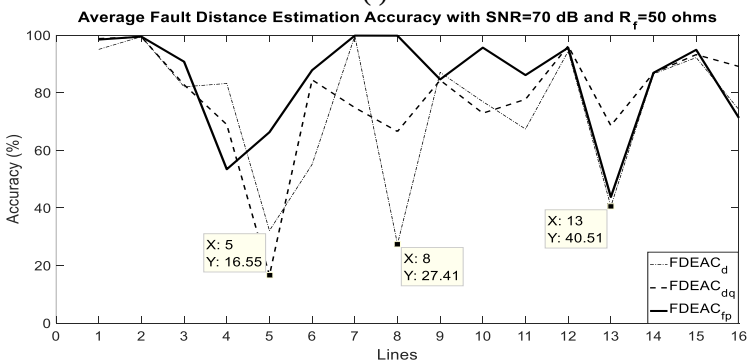

(ii)

Fig. 10. The average fault distance estimation accuracy in all lines with SNR=70dB for (i) Rf=0.001 Ω and (ii) Rf=50 Ω

The performance of overall average fault information acuracy for all specified SNR values is illustrated in Fig. 11 (i) for $0.001\,\Omega$ minimum fault resistance and (ii) for $50\,\Omega$ maximum assumed fault resistance respectively. In this figure, the overall fault information accuracy values gradually increase according to SNR values. The overall average fault information accuracy by proposed algorithm FAC_{fp} can give the highest accuracies for every specified SNR values. This Fig. 11 also confirm that the faulted phase time delay is the most accurate one in these time delays.

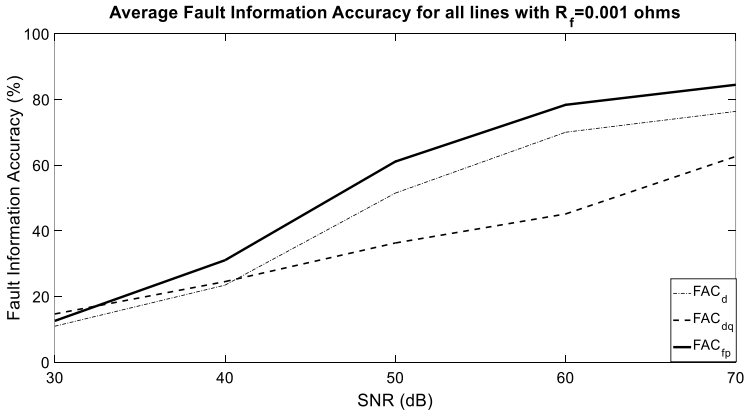

(i)

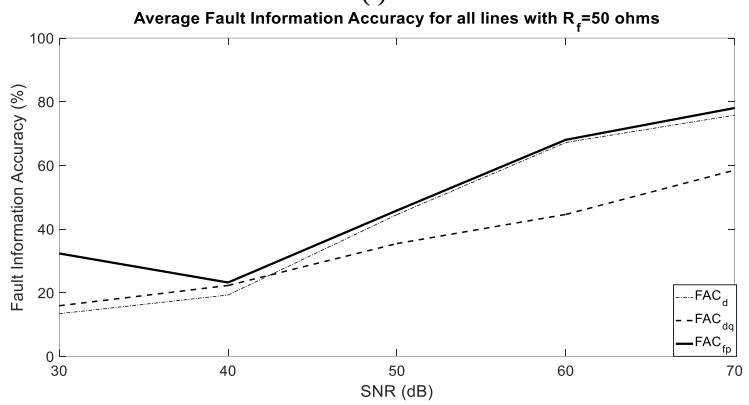

(ii)

Fig. 11. Overall average fault information accuracy in all lines with SNR=30 to 70 dB for (i) $R_f = 0.001\,\Omega$ and (ii) $R_f = 50\,\Omega$

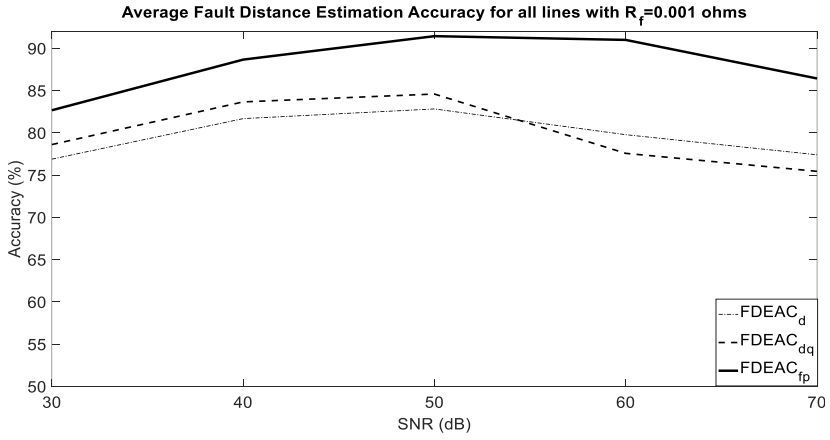

(i)

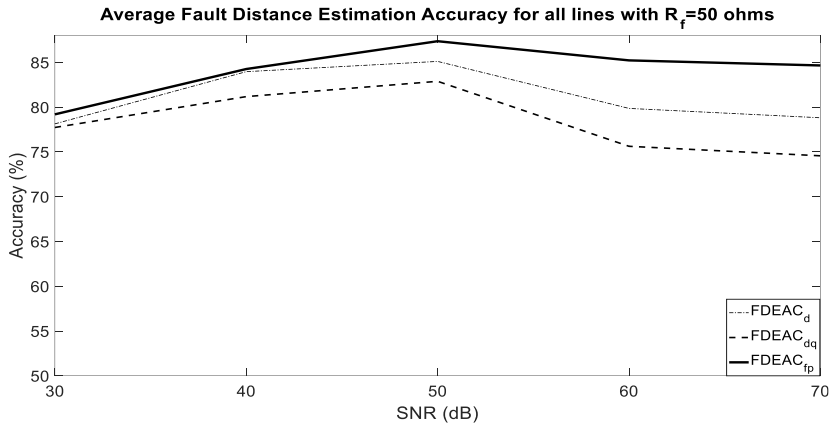

(ii)

Fig. 12. Overall average fault distance estimation accuracy in all lines with SNR= 30 to 70dB for (i) Rf=0.001 Ω and (ii) Rf=50 Ω .

The performance of overall average fault distance estimation acuracy for all specified SNR values is illustrated in Fig. 12 (i) for 0.001 Ω minimum fault resistance and (ii) for 50 Ω maximum assumed fault resistance respectively. According to this figure, the algorithm is performing that how the noise affect the arrival time of the fault signal at the sensing bus.

Fig. 12. compares the overall fault distance estimation accuracy of conventional aerial component, aerial different component and proposed faulted phase-based component. Faulted phase-based algorithm can give the highest accuracies for every specified SNR values because the faulty phase can give more accurate fault information than healthy phases.

8. CONCLUSION

This paper proposes a simple fault localization technique in loop distribution systems. The proposed technique passed through band pass filter, Karenbauer's Transform and Wavelet Transform criteria to estimate for fault distance by using only three phase current signals at the source bus (B_1) of the test distribution network. According to detail level analysis section, using the arriving times of the component combined the three reconstructed signals using three detail level coefficients (D_1, D_2 and D_3) can give best accuracy. The proposed algorithm shows that the faulted phase time delay (Δt_{fp}) can give better accuracy than using conventional time delay (Δt_d)and aerial different time delay (Δt_{dq}).

The algorithm performance is successfully tested with data obtained by simulations with 1650 different cases of sampled data at various situations, faulted feeders, faulted resistance, 30 to 70 dB SNR values and fault locations. The proposed methodology is evaluated through MATLAB Simulation single line to ground fault in a 10-kV grounded loop distribution system. The proposed algorithm can give fault information accuracy up to 100% and fault location accuracy up to 99.7% with 30 dB contaminated SNR for the nearest lines from the measured terminal. Using proposed algorithm, the overall fault information accuracy can get up to 83% and overall fault distance estimation accuracy up to 93%. This proposed technique can be used to implement in real data with actual fault records.

REFERENCES

[1] Y. Liao, "A noval method for locating faults on distribution systems," *Elect; Pow; Syst; Research*, vol. 117, pp. 21 – 26, 2014.
[2] A. C. Adewole, R. Tzoneva, S. Behardien, "Distribution network fault section identification and fault location using wavelet entropy and neural networks," *Applied Soft Computing*, vol. 46, pp. 296–306, 2016.
[3] A. Swetapadma, A. Yadav, "A novel decision tree regression-based fault distance estimation scheme for transmission lines" *IEEE Trans; on Pow; Delivery*, pp. 1-10, 2016.
[4] X. Deng, R. Yuan, Z. Xiao, T. Li, K. L.L.Wang, "Fault location in loop distribution network using SVM technology" *Elec; Pow; and Energ Syst*, vol. 65, pp. 254–261, 2015.
[5] M. Daisy and R. Dashti, "Single phase fault location in electrical distribution feeder using hybrid method," *Energy*, vol. 103, pp. 356–368, 2016.

[6] S. H. Monazavi, Z. Moravej, S. M. Shahrtash, " A searching based method for locating high impedance arcing fault in distribution networks" *IEEE Trans; on Pow; Delivery*, vol. 34, no. 2, pp. 438-447, April 2019.
[7] M. J. S. Ramos, A.S. Bretas, D. P. Bernardon, L. L. Pfitscher, "Distribution network HIF location: A frequency domain system model and WLS parameter estimation approach" *Elect; Pow; Syst; Research*, pp. 170-176, 2017.
[8] P. Cao, H. Shu, B. Yang, J. Dong, Y. Fang, T. Yu, "Speeded-up robust features based single-ended traveling wave fault location: a practical case study in Yunnan power grid of China" *IET Gener. Transm. Distrib.*, vol. 12, iss. 4, pp. 886-894, 2018.
[9] J. Ding, L. Li, Y. Zheng, C. Zhao, H. Chen, X. Wang, "Distributed traveling-wave-based fault location without time synchronization and wave velocity error" *IET Gener. Transm. Distrib.*, vol. 11, iss. 8, pp. 2085-2093, 2017.
[10] S. Shi, B. Zhu, A. Lei, X. Dong, "Fault location for radial distribution network via topology and reclosure-generating traveling waves" *IEEE Trans. Smart Grid*, pp. 1-10, 2019.
[11] J. Sadeh, E. Bakhshizadeh, and R. Kazemzadeh, "A new fault location algorithm for radial distribution systems using modal analysis," *Int. J. Electr. Power Energy Syst.*, vol. 45, no. 1, pp. 271–278, 2013.
[12] R. Liang, F. Wang, G. Fu, X. Xue, and R. Zhou, "A general fault location method in complex power grid based on wide-area traveling wave data acquisition," *Int. J. Electr. Power Energy Syst.*, vol. 83, pp. 213–218, 2016.
[13] B.K. Chaitanya, A. Yadva, "Decision tree aided traveling wave-based fault section identification and location scheme for multi-terminal transmission lines" *Measurement*, vol. 135, pp. 312-322, 2019.
[14] L. Ye, D. You, X. Yin, K. Wang, and J. Wu, "An improved fault-location method for distribution system using wavelets and support vector regression," *Int. J. Electr. Power Energy Syst.*, vol. 55, pp. 467–472, 2014.
[15] Q. Jia, X. Dong, S. Mirsaeidi, "A traveling-wave-based line protection strategy against single-line-to-ground faults in active distribution networks" *Int. J. Electr. Power Energy Syst.*, vol. 107, pp. 403-411, 2019.
[16] L. Rui, F. G.uoqing, Z. Xueyuan, X. Xue, "Fault location based on single terminal traveling wave analysis in radial distribution network" *Int. J. Electr. Power Energy Syst.*, vol. 66, pp. 160-165, 2015.
[17] L. Rui, P. Nan, Y. Zhi, F. Zare, "A novel single-phase-to-earth fault location method for distribution network based on zero-sequence components distribution characteristics", *Electr. Power and Ener. System*, vol. 102, pp. 11-22, 2018.
[18] L Rui, L. Chenglei, P. Nan, C. Menghan and W. Fei. "Fault location for power grid based on transient traveling wave data fusion via asynchronous voltage measurements" *Elec; Pow; Energ Syst*, pp. 426-439, 2017.
[19] C. Zhou, Q. Shu, X. Han, "A single phase earth fault location scheme for distribution feeder on the basic of the difference of zero mode traveling waves" *Int. Trans. Electr. Energ. Syst.*, pp. 1-9, 2016.
[20] S. Myint, W. Wichakool, "A traveling wave-based fault section and fault distance estimation algorithm for grounded distribution systems" *GTD Asia Grand International Conference 2019*, 19-23, March, Bangkok, Thailand.
[21] S. Myint, W. Wichakool, "A High Frequency Reflected Current Signals-Based Fault Type Identification Method", *Indo. J. of Elect. Eng. Comp. Science*, vol 17, iss 2, pp. 551-563, 2020.
[22] S. Myint, W. Wichakool, "Fault type identification method based on wavelet detail coefficients of modal current components", *Proc. of the 2018 IEEE 5th International Conference on Smart Instrumentation*.

BIOGRAPHIES OF AUTHORS
